Characterization of Strip Line Crossing by Transverse Resonance Analysis

TOMOKI UWANO, MEMBER, IEEE, ROBERTO SORRENTINO, SENIOR MEMBER, IEEE, AND TATSUO ITOH, FELLOW, IEEE

Abstract—**A method of analysis is described for characterizing the discontinuities made of two orthogonally crossed strip lines on a suspended substrate. The method of analysis is based on the generalized transverse resonant technique extended here to four-port configurations. The technique is used for determination of resonant structure at a given frequency and subsequently the equivalent circuit parameters of the discontinuities.**

I. Introduction

STRIP LINE CROSSINGS of the multilayer printed circuit board are commonly used in digital circuit design. As the signal frequency gets higher due to high-speed processors, an accurate wave analysis of the characteristics of the crossing becomes important. In addition, the crossing of strips on both sides of the suspended substrate often appears in microwave and millimeter-wave integrated circuits [1]. To date little has been reported on the exact analysis of such structures.

The problem presented here is to characterize the discontinuities of two orthogonally crossed strip lines. The structure to be analyzed is shown schematically in Fig. 1 along with the coordinate system. It is assumed that the structure is lossless. Two strip lines are crossed orthogonally on opposite sides of the substrate. Auxiliary conducting planes are added to convert the structure to a closed one. It is assumed that each pair of opposing side walls does not influence the electromagnetic fields guided by the strip parallel to the walls but only the field guided along the orthogonal directions. This assumption is valid as long as the field remains confined in the proximity of the two strip lines. Thus, surface wave and radiation phenomena are excluded. The auxiliary walls are used for field analysis purposes. They permit the structure to be analyzed as a rectangular waveguide discontinuity problem.

The method of analysis is based on the generalized "transverse resonance technique" introduced for finline step discontinuity problems [2]. The technique is extended here to a four-port configuration treated in this paper. The method consists of two parts. First, the resonant structure created by auxiliary walls is described in terms of network representation containing a reactive four-port. For a fixed resonant frequency, we try to find as many resonator configurations as required for extraction of four-port matrix elements. The second part of the analysis is a full-wave electromagnetic field analysis in which the resonant frequency is found as an eigenvalue problem. In this part of the analysis, the problem is viewed as one of waveguide scattering for waves traveling in the direction normal to the substrate surface.

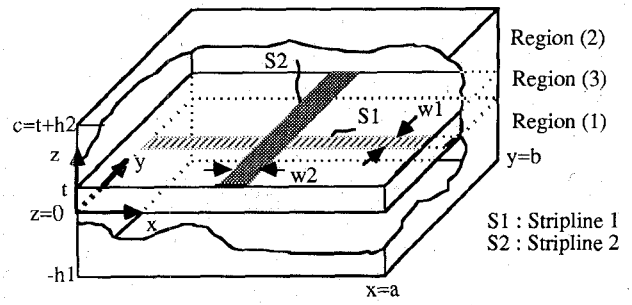

Fig. 1. Structure of the problem.

II. Circuit Representation

In this section, a procedure for a two-port resonance method [3] is extended to a four-port configuration. The crossing between the two suspended strip lines can be represented as a four-port network at some reference planes. Reference planes can be placed at any position as long as they are on the continuous part of the transmission line. Each port is terminated with a reactance corresponding to the line section between the reference plane and the auxiliary wall, as shown in Fig. 2. The network equations for the entire circuit are expressed in matrix form as

$$[[Z]+\mathrm{diag}[Zi]][I]=0 \qquad (1)$$

where $[Z]$ is the impedance matrix of the four-port network normalized with respect to the characteristic impedance at each port. $Zi(i=1,2,3,4)$ are the normalized terminal impedances: $Zi=j\tan\beta li_i$, with $li(i=1,2,3,4)$ the strip line lengths between the reference planes and the auxiliary walls. $[I]$ is the vector of the currents $Ii(i=1,2,3,4)$ as shown in Fig. 2. In the absence of losses, $[Z]$ is imaginary and the resonant frequency is real. The resonant frequency

Manuscript received February 18, 1987; revised July 13, 1987. This work was supported in part by the Office of Naval Research under Contract N00014-79-C-0553.

T. Uwano was with the Department of Electrical Engineering, University of Texas at Austin, Austin, TX 78712, on leave from the Matsushita Electric Ind. Co., Ltd., Osaka 571, Japan.

R. Sorrentino is with the Department of Electrical Engineering, University of Rome Tor Vergata, 00173 Rome, Italy.

T. Itoh is with the Department of Electrical Engineering, University of Texas at Austin, Austin, TX 78712.

IEEE Log Number 8717241.

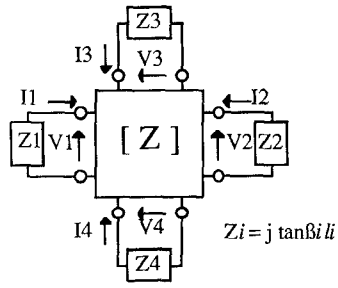

Fig. 2. Four-port network for the problem.

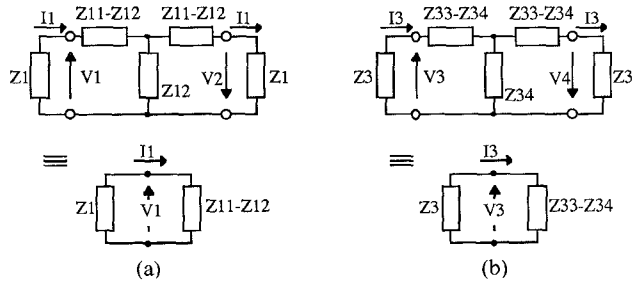

Fig. 3. Equivalent circuits for an odd resonance. (a) Strip 1. (b) Strip 2.

is obtained from the condition that the voltages and currents be nontrivial in the absence of sources. From (1), this condition is

$$\det \| [Z] + \operatorname{diag}[Zi] \| = 0. \tag{2}$$

The values of the Zi's can be specified once the distance to the wall is fixed while the Z parameters are to be determined. The impedance matrix of a reciprocal four-port lossless network possesses in general ten independent imaginary parameters. In the present case, however, because of the symmetry of the structure, only five parameters are needed to characterize the Z matrix:

$$\begin{bmatrix} V1 \\ V2 \\ V3 \\ V4 \end{bmatrix} = \begin{bmatrix} Z11 & Z12 & Z13 & Z13 \\ Z12 & Z11 & Z13 & Z13 \\ Z13 & Z13 & Z33 & Z34 \\ Z13 & Z13 & Z34 & Z33 \end{bmatrix} \begin{bmatrix} I1 \\ I2 \\ I3 \\ I4 \end{bmatrix}. \tag{3}$$

From (3), the resonant condition of (2) can be written in the following form:

$$\begin{aligned} &\{(Z11+Z1)(Z11+Z2)-Z12^2\} \\ &\cdot\{(Z33+Z3)(Z33+Z4)-Z34^2\} \\ &\cdot -4Z13^2\{Z11-Z12+(Z1+Z2)/2\} \\ &\cdot\{Z33-Z34+(Z3+Z4)/2\}=0. \end{aligned} \tag{4}$$

Now we can show that by properly choosing the terminal impedance Zi's, the resonant conditions are simplified so that the problem is solved analytically. First, let us choose the terminal impedances in a symmetrical way, i.e., $I1 = I2$ and $I3 = I4$ so that $Z1 = Z2$ and $Z3 = Z4$. If these conditions are applied, (4) can be factorized in the form

$$\begin{aligned} &(Z11+Z1-Z12)(Z33+Z3-Z34) \\ &\cdot\{(Z11+Z12+Z1)(Z33+Z34+Z3)-4Z13^2\}=0. \end{aligned} \tag{5}$$

Thus

$$Z11+Z1-Z12=0 \tag{6}$$

or

$$Z33+Z3-Z34=0 \tag{7}$$

or

$$(Z11+Z12+Z1)(Z33+Z34+Z3)-4Z13^2=0. \tag{8}$$

With each factor in (5) equated to zero, the eigenvalues for the matrix in (1) are obtained; each eigenvalue ω is then the resonant frequency under the condition of the corresponding eigenvector of the currents. When the first factor in (5) is equated to zero, i.e., (6) is satisfied, the eigenvector of (1) is $I1 = -I2$ and $I3 = I4 = 0$. This condition corresponds to the odd resonance of the structure shown in Fig. 3(a). The structure behaves as if an electric wall were placed symmetrically along the center of strip line 2. For the given resonant frequency, the required resonance condition provides the quantity $Z11 - Z12$ for a given value of $Z1$. Similarly, when (7) is satisfied, an odd resonance of strip line 2 is obtained, and the structure for this condition is shown in Fig. 3(b). Finally, from (8), the eigenvector for an even resonance is obtained: $I1 = I2$ and $I3 = I4$. Substitution of these conditions into (3) yields the two-port network matrix equation

$$\begin{bmatrix} V1 \\ V3 \end{bmatrix} = \begin{bmatrix} Z11+Z122 & Z13 \\ 2Z13 & Z33+Z34 \end{bmatrix} \begin{bmatrix} I1 \\ I3 \end{bmatrix}. \tag{9}$$

The use of symmetry, therefore, has reduced the four-port network problem to that of a two-port. For a given resonant frequency, three different pairs of $Z1$ and $Z3$ (with $Z1 = Z2$ and $Z3 = Z4$) are used to provide three quantities $Z11'$, $Z12'$ and $Z22'$ which denote the elements of the matrix in (9):

$$Z11' = Z11 + Z12 \tag{10}$$

$$Z22' = Z33 + Z34 \tag{11}$$

$$Z12' = 2Z13. \tag{12}$$

Combining the results with those for the two structures in Fig. 3, we obtain all five Z parameters. For the procedure illustrated above, we must know the propagation constants of the two isolated strip lines, i.e., $\beta 1$ and $\beta 3$. The quantities are necessary to obtain $Z1$ and $Z3$:

$$Z1 = j \tan \beta 1 (a - w2)/2 \tag{13}$$

$$Z3 = j \tan \beta 3 (b - w1)/2. \tag{14}$$

These expressions are obtained for a specific choice of the reference planes, as shown in Fig. 4. As the reference planes are placed close to the discontinuity, negative capacitors or inductors may appear in an equivalent circuit representation. The field analysis can be also used to determine $\beta 1$ and $\beta 3$. This can be done simply by setting $\beta 1 = \pi/a$ and $\beta 3 = \pi/b$ at a specified resonant frequency for the isolated strip line.

It is important to find an equivalent circuit representation of the four-port structure so that it is most

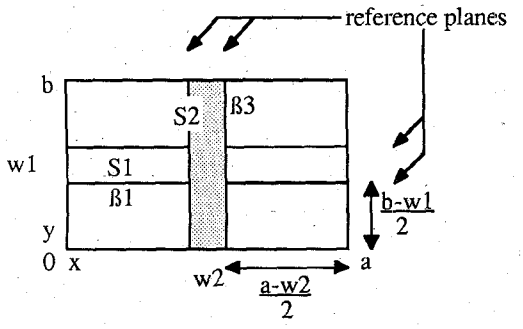

Fig. 4. A choice of reference plane (top view).

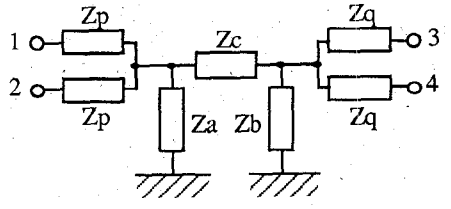

Fig. 5. Equivalent circuit for the problem.

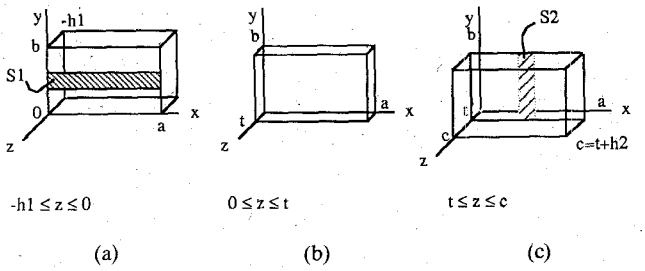

Fig. 6. Subregions for fields analysis. (a) Region (1). (b) Region (3). (c) Region (2).

convenient for the present analysis. For the structure in Fig. 1, one possible equivalent circuit representation could be chosen as shown in Fig. 5. The circuit already takes the symmetry properties into account. Zc is used to represent the coupling capacitance between the two strips. $Zp + Zp$ and $Zq + Zq$ represent the inductances associated with the two strip line sections, while Za and Zb represent the two strip-to-ground capacitances.

The S matrix for a four-port network is obtained from the relation

$$[S] = [[Z]+[U]]^{-1}[[Z]-[U]] \tag{15}$$

where $[U]$ is a unit matrix.

III. Field Analysis

The resonant structure of Fig. 1 can be subdivided into three homogeneous regions as shown in Fig. 6. In terms of the TE-to-z and TM-to-z representations, the hybrid fields in each homogeneous region in the resonator structure are as follows:

region (1): $h1 \leqslant z \leqslant 0$

$$Et^{(1)} = -\sum_m^M \sum_n^N \left[Amn^{(1)} \nabla t \psi mn \times z + Bmn^{(1)} \left(\beta mn^{(1)} / \hat{y}_1 \right) \nabla t \varphi mn \right] \sin \beta mn^{(1)} (z + h1) \tag{16}$$

$$Ht^{(1)} = \sum_m^M \sum_n^N \left[Amn^{(1)} \left(\beta mn^{(1)} / \hat{z}_1 \right) \nabla t \psi mn + Bmn^{(1)} \nabla t \varphi mn \times z \right] \cos \beta mn^{(1)} (z + h1) \tag{17}$$

region (2): $t \leqslant z \leqslant c$

$$Et^{(2)} = -\sum_m^M \sum_n^N \left[Amn^{(2)} \nabla t \psi mn \times z + Bmn^{(2)} \left(\beta mn^{(2)} / \hat{y}_2 \right) \nabla t \varphi mn \right] \sin \beta mn^{(2)} (z - c) \tag{18}$$

$$Ht^{(2)} = \sum_m^M \sum_n^N \left[Amn^{(2)} \left(\beta mn^{(2)} / \hat{z}_2 \right) \nabla t \psi mn + Bmn^{(2)} \nabla t \varphi mn \times z \right] \cos \beta mn^{(2)} (z - c) \tag{19}$$

region (3): $0 \leqslant z \leqslant t$

$$Et^{(3)} = -\sum_m^M \sum_n^N \left[\left\{ Cmn \sin \beta mn^{(3)} z + Dmn \sin \beta mn^{(3)} (z - t) \right\} \nabla t \psi mn \times z + \left\{ Fmn \sin \beta mn^{(3)} z + Gmn \sin \beta mn^{(3)} (z - t) \right\} \cdot \left(\beta mn^{(3)} / \hat{y}_3 \right) \nabla t \varphi mn \right] \tag{20}$$

$$Ht^{(3)} = \sum_m^M \sum_n^N \left[\left\{ Cmn \cos \beta mn^{(3)} z + Dmn \cos \beta mn^{(3)} (z - t) \right\} \cdot \left(\beta mn^{(3)} / \hat{z}_3 \right) \nabla t \psi mn + \left\{ Fmn \cos \beta mn^{(3)} z + Gmn \cos \beta mn^{(3)} \cdot (z - t) \right\} \nabla t \varphi mn \times z \right] \tag{21}$$

where

$$\psi mn = Pmn \cos\left(\frac{m\pi x}{a}\right) \cos\left(\frac{n\pi y}{b}\right)$$

$$\varphi mn = Pmn \sin\left(\frac{m\pi x}{a}\right) \sin\left(\frac{n\pi y}{b}\right)$$

$$Pmn = \sqrt{\frac{\delta m \delta n}{ab}} \frac{1}{kc}, \qquad \delta i = \begin{cases} 1, & i = 0 \\ 2, & i \neq 0 \end{cases}$$

$$kc^2 = \left(\frac{m\pi}{a}\right)^2 + \left(\frac{n\pi}{b}\right)^2$$

$$\beta mn^{(i)} = \left(k_i^2 - kc^2\right)^{1/2}, \qquad i = 1,2,3$$

$$\hat{y}_i = j\omega\epsilon_i \qquad \hat{z}_i = j\omega\mu_i \qquad k_i^2 = -\hat{y}_i \hat{z}_i$$

where $Amn^{(1)}$, $Amn^{(2)}$, $Bmn^{(1)}$, $Bmn^{(2)}$, Cmn, Dmn, Fmn, and Gmn are unknown coefficients, z is a z-directional

unit vector, and the superscripts in parentheses refer to the respective regions.

The boundary conditions at each interface are as follows:

interface (I): at $z = 0$

$$Et_1 = Et_3 \qquad \text{on } S \tag{22}$$

$$Et_1 = Et_3 = 0 \qquad \text{on } S1 \tag{23}$$

$$Ht_3 - Ht_1 = \begin{cases} \Delta Ht^{(1)} & \text{on } S1 \\ 0 & \text{on } S - S1 \end{cases} \tag{24}$$

interface (II): at $z = t$

$$Et_2 = Et_3 \qquad \text{on } S \tag{25}$$

$$Et_2 = Et_3 = 0 \qquad \text{on } S2 \tag{26}$$

$$Ht_2 - Ht_3 = \begin{cases} \Delta Ht^{(2)} & \text{on } S2 \\ 0 & \text{on } S - S2 \end{cases} \tag{27}$$

where $\Delta Ht^{(i)} (i = 1,2)$ are unknown functions of x, y. These functions are expanded in terms of a set of known orthogonal vector functions $\chi\nu^{(i)}$ defined over Si with unknown coefficients $P\nu^{(i)}$:

$$\Delta Ht^{(1)} = \sum_{\nu} P\nu^{(1)} \chi\nu^{(1)} \tag{28}$$

$$\Delta Ht^{(2)} = \sum_{\nu} P\nu^{(2)} \chi\nu^{(2)}. \tag{29}$$

Inserting (16) ~ (21) into (22) ~ (27) and making use of the orthogonal properties of $\nabla t\psi mn$ and $\nabla t\varphi mn$, we obtain a homogeneous system of equations in terms of the unknown coefficient $P\nu$:

$$\sum_{\nu_1}^{\nu_{1M}} P\nu^{(1)} U\mu\nu^{(11)} + \sum_{\nu_2}^{\nu_{2M}} P\nu^{(2)} U\mu\nu^{(12)} = 0, \quad \mu = 1,2,3,\ldots,\nu_{1M} \tag{30}$$

$$\sum_{\nu_1}^{\nu_{1M}} P\nu^{(1)} U\mu\nu^{(21)} + \sum_{\nu_2}^{\nu_{2M}} P\nu^{(2)} U\mu\nu^{(22)} = 0, \quad \mu = 1,2,3,\ldots,\nu_{2M} \tag{31}$$

where

$$U\mu\nu^{(ij)} = \sum_{m}^{M} \sum_{n}^{N} S_i \left\{ amn^{(ij)} \xi mn, \mu^{(i)} \xi mn, \nu^{(j)} - \left(\beta^{(i)} / \hat{y}_i\right) bmn^{(ij)} \theta mn, \mu^{(i)} \theta mn, \nu^{(j)} \right\}, \quad i, j = 1,2 \tag{32}$$

$$\xi mn, \mu^{(i)} = \int_{Si} \chi\mu^{(i)} \cdot \nabla t\psi mn \, ds, \qquad i = 1,2$$

$$\theta mn, \mu^{(i)} = \int_{Si} \chi\mu^{(i)} \cdot \nabla t\varphi mn \times z \, ds, \qquad i = 1,2.$$

The quantities $amn^{(ij)}$, $bmn^{(ij)}$, $\xi mn, \mu$, and $\theta mn, \mu$ are described in the Appendix.

The condition for nontrivial solution determines the characteristic equation of the given structure. This equation may be regarded as a function of $\omega, l1, l3$, equated to zero:

$$f(\omega, l1, l3) = 0. \tag{33}$$

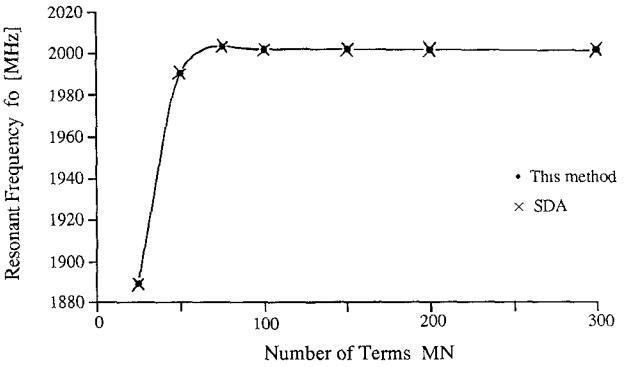

Fig. 7. Convergence of the resonant frequency of an isolated strip line.

For a given value of $\omega = \omega_r$, (33) can be solved to evaluate the different pairs of $l1$ and $l3$ giving rise to the same resonant frequency ω_r. These values of $l1$ and $l3$ can be used for computing the discontinuity parameters discussed in the previous section.

IV. Computed Results

In accordance with the technique described above, the electromagnetic fields in each region are expressed in terms of the series expansions. In the numerical computation, only a finite number of terms can be retained in the series expansions. The number of terms was chosen in such a way that the highest spatial frequencies of the electromagnetic field are approximately the same in the transverse directions (x, y). The current on a strip line is expanded in such a way that the distributions of each component (Jx, Jy) in the transverse direction are expressed by only the first term and that the distributions in the longitudinal direction are expressed by a set of terms, the number of which is the same on each strip line.

The method is first tested by computing the resonant frequency of the isolated strip line with certain structural parameters. Fig. 7 shows the convergence of the resonant frequency with respect to the number of terms of the field expansions in the homogeneous region of Fig. 6. The numbers M, N were chosen to be the same in both the x and y directions. The results exhibit very good agreement with those by the spectral domain approach [4] in which the resonant frequency was calculated from the propagation constant. The field was represented by the same number of harmonics in both this method and the spectral domain approach. Fig. 8 shows the convergence of the resonant frequency of the crossing strip line structure with respect to the number ν of current expansion terms in the longitudinal direction. From Fig. 8, we could observe a fast convergence characteristic with a relatively small number of current expansions if the electromagnetic field is well expressed by an adequate number of harmonics.

In the computations, the substrate was placed symmetrically between the top and bottom planes with both strips having the same widths. Hence, the impedance matrix representation of the discontinuities has $Z11 = Z33$ and $Z12 = Z34$. The element values for the equivalent circuit calculated at three different frequencies are quoted in

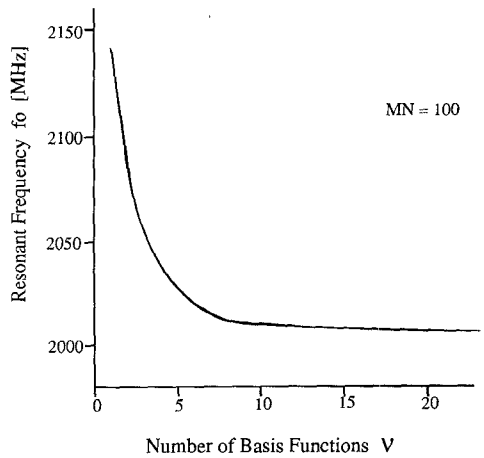

Fig. 8. Convergence of the resonant frequency of crossing strip lines.

TABLE I
ELEMENT VALUES OF EQUIVALENT CIRCUIT

	0.5 GHz	1 GHz	2 GHz
Lp=Lq	0.331nH	0.331nH	0.329nH
Ca=Cb	-0.0885pF	-0.103pF	-0.101pF
Cc	0.249pF	0.272pF	0.258pF
MN	400	200	100
V	20	20	20

$$Lp = Lq = \frac{Z0Zp}{j\omega}.$$

$$Ca = Cb = \frac{1}{j\omega Z0Za}.$$

$$Cc = \frac{1}{j\omega Z0Zc}.$$

Zp, Zq, Za, Zb, Zc: normalized impedance.
$Z0$: Strip line characteristic impedance (159.2,159.1,158.3 Ω at 0.5,1,2 GHz).
$h1 = h2 = 5$ mm; $t = 1$ mm.
$w1 = w2 = 1$ mm; $\epsilon_r = 3.8$.

Table I, along with the structural parameters used in the computations, where the reference planes were defined in the same manner as in Fig. 4. Fig. 9 shows the corresponding S parameters of the discontinuities. Note that the elements for Za and $Zb(=Za)$ are capacitors with a negative value. This is acceptable because they compensate the parallel distributed capacitance for the isolated strip line in the absence of the other strip line. In other words, the strip-to-ground capacitance of the line section between ports 1 and 2 becomes positive with the combination of Za, Zb, Zc and the fringingcapacitances at the open ports 3 and 4. The uniqueness of the solution with respect to the different sets of $\{l1, l2, l3, l4\}$ was also tested, and the same results were obtained with an accuracy better than that by the convergence.

Zc was also calculated with $h1 = 10$ mm, $h2 = 100$ mm, $t = 5$ mm, $w1 = w2 = 0.4$ mm, $\epsilon_r = 1$ at 2 GHz, simulating the crossing model of the work by *Giri et al.* [5]. The result

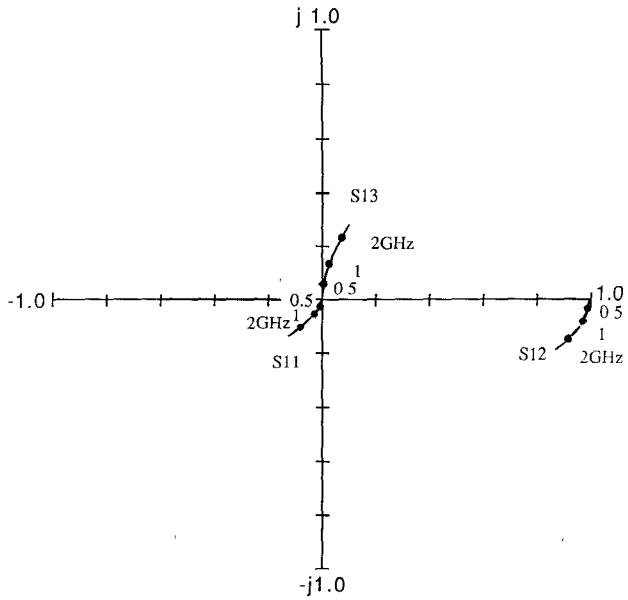

Fig. 9. S parameters of the discontinuities of the structure.

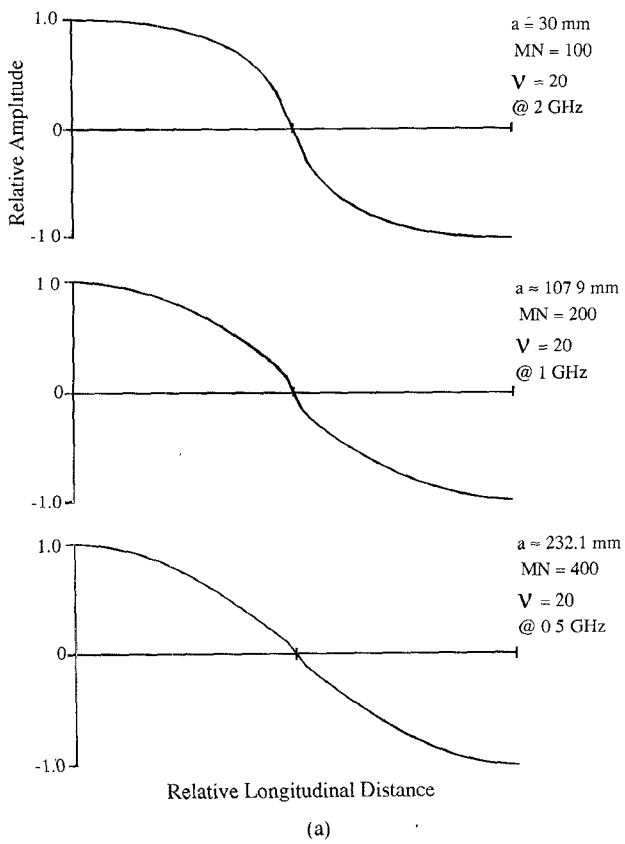

(a)

Fig. 10. Current distribution on the strip line. (a) Longitudinal current. (b) Transverse current (*continued on next page*)

for the value of Cc was 0.082 pF, while the value of the coupling capacitor Cm as defined in [5] was estimated to be 0.15 pF by using the equivalent radius.

Fig. 10(a) and (b) shows the longitudinal and transverse components of the current densities at the center of the strip at the three different frequencies. In Fig 10(a), it is observed that each figure was of perturbed cosine form.

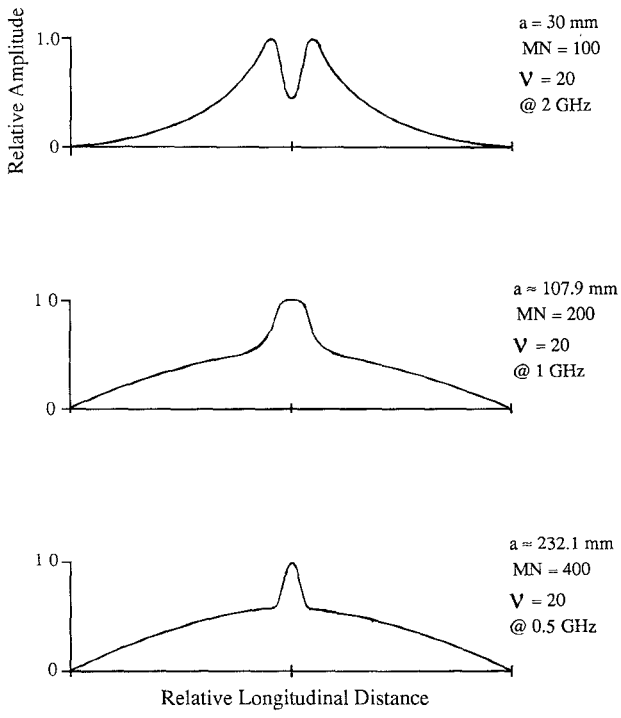

(b)

Fig. 10. (*Continued*).

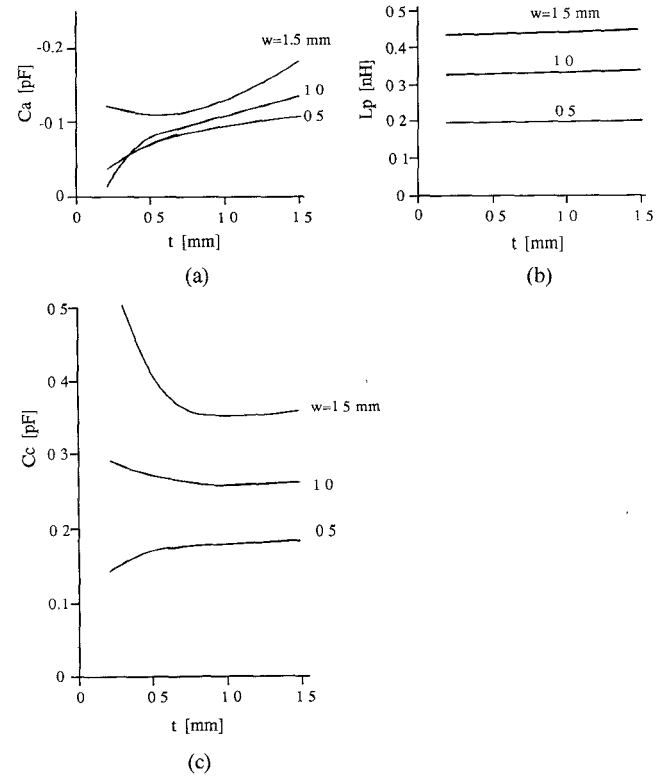

Fig. 11. Element values versus strip line width and substrate thickness. (a) *Ca*. (b) *Lp*. (c) *Cc*.

This feature is anticipated from an observation that the strip line whose length is slightly shorter than half a wavelength turns out to be a resonator with capacitive loading at the center of the strip line. The longitudinal current may therefore be represented by the combination of a cosine and an additional polynomial function [6] so that the computation time can be reduced. As to the transverse current shown in Fig. 10(b), the figures are not readily characterized. This implies that the current function requires a number of terms of basis functions.

Fig. 11(a), (b), and (c) shows the computed results for different values of the strip line width and the substrate thickness.

V. Conclusions

A method of analysis has been described for characterizing the discontinuities of two crossed strip lines. The method is based on the generalized transverse resonance technique for computing the resonant frequency of a resonator created by enclosing the crossing with perfectly conducting auxiliary walls. This resonator problem is analyzed as one of waveguide scattering for waves traveling in the direction normal to the substrate surface. For a specified frequency, resonant structures are found by adjusting the lengths of the strips and hence the resonator size. These structures are used for deriving the equivalent circuit parameters characterizing the discontinuity.

This method can also be applied for the characterization of strip line–slotline transition.

Appendix

A. Derivation of Elements in Fig. 5

The relations between the elements of (3) and the normalized impedances of the equivalent circuit in Fig. 5 are

$$Z11 = Zp + \frac{Za(Zb + Zc)}{Za + Zb + Zc}$$

$$Z12 = \frac{Za(Zb + Zc)}{Za + Zb + Zc}$$

$$Z13 = \frac{ZaZb}{Za + Zb + Zc}$$

$$Z33 = Zq + \frac{Zb(Zc + Za)}{Za + Zb + Zc}$$

$$Z34 = \frac{Zb(Zc + Za)}{Za + Zb + Zc}.$$

Hence

$$Za = \frac{Z13^2 - Z12Z34}{Z13 - Z34}$$

$$Zb = \frac{Z13^2 - Z12Z34}{Z13 - Z12}$$

$$Zc = -\frac{Z13^2 - Z12Z34}{Z13}$$

$$Zp = Z11 - Z12$$

$$Zq = Z33 - Z34.$$

B. Derivation of (32)

The H field on the strip is expanded in terms of known basis functions $\chi\nu$ with unknown coefficients $P\nu$. Actually, what will be expanded is the H field discontinuity which is equal to $Jt \times z$, viz.,

$$\Delta Ht = \sum_{\nu}^{\nu \max} P\nu\chi\nu = Jt \times z.$$

The basis functions are chosen in such a way that the field is nonzero only on the strip. Additional boundary conditions must be satisfied at the strip ends where the strip lines are terminated with electric walls. The field may be expanded in terms of the basis functions of two different types. One of them consists of harmonic basis functions, the other of singular basis functions. The singular behavior of the magnetic field component normal to the strip line edges is incorporated in the singular basis functions. They are therefore expected to provide a faster numerical convergence.

For the H field expansion on $S1$, the following set is employed:

$$\chi^{(1)}_{x,rs} = \sin\frac{r\pi x}{a}\sin\left[\frac{s\pi}{w1}\left\{y - \frac{(b-w1)}{2}\right\}\right]$$

$$\chi^{(1)}_{y,rs} = \cos\frac{r\pi x}{a}\frac{\cos\left[\frac{s\pi}{w1}\left\{y - \frac{(b-w1)}{2}\right\}\right]}{\sqrt{1' - \left\{\frac{(y-b/2)}{w1/2}\right\}^2}}$$

where the subscript rs is used instead of n for representing the variations in the two orthogonal directions. Similar expansions are employed for the H field on $S2$.

The quantities in (32) are as follows:

$$amn^{(11)} = Ka(1/S_1)\left(\beta^{(2)}Ct_2 + \beta^{(3)}Ct_3\right)$$
$$amn^{(12)} = Ka(1/(S_1S_3))\beta^{(3)}$$
$$amn^{(21)} = -Ka(1/(S_2S_3))\beta^{(3)}$$
$$amn^{(22)} = -Ka(1/S_2)\left(\beta^{(1)}Ct_1 + \beta^{(3)}Ct_3\right)$$
$$Ka = \hat{z}/\left\{\beta^{(3)2} - \beta^{(3)}Ct_3\left(\beta^{(2)}Ct_2 + \beta^{(1)}Ct_1\right) - \beta^{(1)}\beta^{(2)}Ct_1Ct_2\right\}$$
$$bmn^{(11)} = Kb(1/S_1)\left(\beta^{(3)}Ct_2 + (\epsilon_3/\epsilon_2)\beta^{(2)}Ct_3\right)$$
$$bmn^{(12)} = Kb(1/(S_1S_3))(\epsilon_3/\epsilon_2)\beta^{(2)}$$
$$bmn^{(21)} = -Kb(1/(S_2S_3))(\epsilon_3/\epsilon_1)\beta^{(1)}$$
$$bmn^{(22)} = -Kb(1/S_2)\left(\beta^{(3)}Ct_1 + (\epsilon_3/\epsilon_1)\beta^{(1)}Ct_3\right)$$
$$Kb = \beta^{(3)}/\left[(\epsilon_3/\epsilon_1)(\epsilon_3/\epsilon_2)\beta^{(1)}\beta^{(2)} - \beta^{(3)}Ct_3 \cdot\left\{(\epsilon_3/\epsilon_1)\beta^{(1)}Ct_2 + (\epsilon_3/\epsilon_2)\beta^{(2)}Ct_1\right\} - \beta^{(3)2}Ct_1Ct_2\right]$$
$$S_1, S_2, S_3 = \sin\beta^{(1)}h1, \sin\beta^{(2)}h2, \sin\beta^{(3)}t$$
$$C_1, C_2, C_3 = \cos\beta^{(1)}h1, \cos\beta^{(2)}h2, \cos\beta^{(3)}t$$
$$Ct_1, Ct_2, Ct_3 = C_1/S_1, C_2/S_2, C_3/S_3$$
$$\hat{z} = jw\mu_0$$
$$\xi x^{(1)} = -Pmn\frac{m\pi}{a}\frac{a}{2}\delta rmHI(s,n,w1,b)$$
$$\xi y^{(1)} = -Pmn\frac{n\pi}{b}\frac{a}{\delta m}\delta rmSI(s,n,w1,b)$$
$$\xi x^{(2)} = -Pmn\frac{m\pi}{a}\frac{b}{\delta n}\delta snSI(r,m,w2,a)$$
$$\xi y^{(2)} = -Pmn\frac{n\pi}{b}\frac{b}{2}\delta snHI(r,m,w2,a)$$
$$\theta x^{(1)} = Pmn\frac{n\pi}{b}\frac{a}{2}\delta rmHI(s,n,w1,b)$$
$$\theta y^{(1)} = -Pmn\frac{m\pi}{a}\frac{a}{\delta m}\delta rmSI(s,n,w1,b)$$
$$\theta x^{(2)} = Pmn\frac{n\pi}{b}\frac{b}{\delta n}\delta snSI(r,m,w2,a)$$
$$\theta y^{(2)} = -Pmn\frac{m\pi}{a}\frac{b}{2}\delta snHI(r,m,w2,a)$$
$$\delta ij = \begin{cases} 0, & i \neq j \\ 1, & i = j \end{cases}$$

$$HI(s,n,w1,b)$$
$$\begin{cases} = \dfrac{w1}{2}\sin\dfrac{(s-n)\pi}{2} & \text{for } \dfrac{n}{b} = \dfrac{s}{w1} \\ = \dfrac{(s\pi T/w1)}{(s\pi/w1)^2 - (n\pi/b)^2}\left[\cos\dfrac{n\pi(b-w1)}{2b} - (-1)^{-s}\cos\dfrac{n\pi(b+w1)}{2b}\right] & \text{for } \dfrac{n}{b} \neq \dfrac{s}{w1} \end{cases}$$

$$SI(s,n,w1,b)$$
$$\begin{cases} = 0 & n+s\text{: even} \\ = \dfrac{\pi w1}{4}\left[\dfrac{(n-s-1)}{(-1)^2}Jo\left(\left|\left(\dfrac{n\pi}{b} - \dfrac{s\pi}{w1}\right)\dfrac{w1}{2}\right|\right) + \dfrac{(n+s-1)}{(-1)^2}Jo\left(\left|\left(\dfrac{n\pi}{b} + \dfrac{s\pi}{w1}\right)\dfrac{w1}{2}\right|\right)\right] & n+s\text{: odd} \end{cases}$$

REFERENCES

[1] H. Ogawa, M. Aikawa, and K. Morita, "*K*-band integrated double-balanced mixer," *IEEE Trans. Microwave Theory Tech.*, vol. MTT-28, pp. 180–185, Mar. 1986.

[2] R. Sorrentino and T. Itoh, "Transverse resonance analysis of finline discontinuities," *IEEE Trans. Microwave Theory Tech.*, vol. MTT-32, pp. 1633–1984, Dec. 1984.

[3] R. E. Collin, *Field Theory of Guided Waves*. New York: McGraw-Hill, 1960.

[4] T. Itoh and R. Mittra, "A technique for computing dispersion characteristics of shielded microstrip lines," *IEEE Trans. Microwave Theory Tech.*, vol. MTT-22, pp. 896–898, Oct. 1974

[5] D. V. Giri, S. H. Chang, and F. M. Tesche, "A coupling model for a pair of skewed transmission lines," *IEEE Trans. Electromagn. Compat.*, vol. EMC-22, pp. 20–28, Feb. 1980.

[6] R. Jansen, "Hybrid mode analysis of end effects of planar microwave and millimetrewave transmission lines," *Proc. Inst. Elec. Eng.*, vol. 128, pt. H, no. 2, pp. 77–86, Apr. 1981.

✠

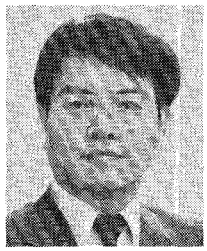

Tomoki Uwano (M'87) was born in Toyama, Japan, on October 18, 1948. He received the B.S. degree from the Tokyo Institute of Technology in 1971.

Since 1971, he has been employed by the Matsushita Electric Ind. Co., Ltd, Osaka, Japan, where he has been engaged in research and development on microwave and millimeter-wave circuitry and satellite communication. From April 1985 to December 1986, he was a Visiting Scholar in the Department of Electrical and Computer Engineering of the University of Texas at Austin.

Mr. Uwano is a member of the Institute of Electronics, Information and Communication Engineers of Japan.

✠

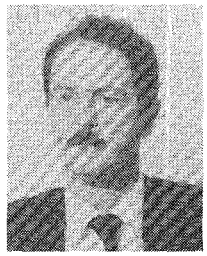

Roberto Sorrentino (M'77–SM'84) received the "Laurea" degree in electronic engineering from the University of Rome "La Sapienza," Rome, Italy, in 1971.

In 1971 he joined the Department of Electronics at the same University, where he was an Assistant Professor of Microwaves. He was also an Associate Professor of Microwaves at the University of Catania, Catania, Italy (1975–76) and at the University of Ancona, Ancona, Italy (1976–77). From 1977 to 1986 he was with the University of Rome "La Sapienza" as an Associate Professor of Solid State Electronics (1977–1981) and Microwave Measurements (1981–1986). In 1983 and 1986 he was appointed a Research Fellow at the University of Texas at Austin, Austin. Since 1986 he has been a Full Professor of Microwaves at the University of Rome "Tor Vergata." His research activities have been concerned with electromagnetic wave propagation in anisotropic media, interaction of electromagnetic fields with biological tissues, and mainly with the analysis and design of microwave and millimeter-wave integrated circuits. In particular, he has contributed to the development of the planar-circuit approach to the analysis of microstrip circuits and to numerical techniques for the characterization of discontinuities in planar and quasi-planar configurations.

Since 1978, Dr. Sorrentino has been involved in many IEEE activities and was Chairman of the Middle and South Italy Section (1984–1987). He founded the local MTT Chapter and served as Chapter Chairman from 1984 to 1987. He is also a member of the Italian Electrical Society (AEI).

✠

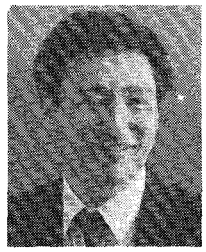

Tatsuo Itoh (S'69–M'69–SM'74–F'82) received the Ph.D. degree in electrical engineering from the University of Illinois, Urbana, in 1969.

From September 1966 to April 1976, he was with the Electrical Engineering Department, University of Illinois. From April 1976 to August 1977, he was a Senior Research Engineer in the Radio Physics Laboratory, SRI International, Menlo Park, CA. From August 1977 to June 1978, he was an Associate Professor at the University of Kentucky, Lexington. In July 1978, he joined the faculty at the University of Texas at Austin, where he is now a Professor of Electrical and Computer Engineering and Director of the Electrical Engineering Research Laboratory. During the summer of 1979, he was a guest researcher at AEG-Telefunken, Ulm, West Germany. Since September 1983, he has held the Hayden Head Centennial Professorship of Engineering at the University of Texas. Since September 1984, he has been the Associate Chairman for Research and Planning in the Electrical and Computer Engineering Department.

Dr. Itoh is a member of the Institute of Electronics and Communication Engineers of Japan, Sigma Xi, and Commissions B and D of USNC/URSI. He served as the Editor of IEEE TRANSACTIONS ON MICROWAVE THEORY AND TECHNIQUES for 1983–1985. He serves on the Administrative Committee of the IEEE Microwave Theory and Techniques Society. Dr. Itoh is a Professional Engineer registered in the state of Texas.